INVESTIGATION OF METHODS FOR MODELING LIGHT PROPAGATION IN MULTILAYER BIOLOGICAL TISSUES FOR CALCULATING THE ABSORBED DOSE OF LASER RADIATION

Krivetskaya A.A.[1,2], Savelieva T.A.[1,2], Kustov D.M.[1], Levkin V.V.[3], Kharnas S.S.[3], Loschenov V.B.[1,2]
[1]Prokhorov General Physics Institute of the Russian Academy of Sciences, Moscow, Russia
[2]Institute of Engineering Physics for Biomedicine, National Research Nuclear University MEPhI, Moscow, Russia
[3]Department of Faculty Surgery No. 1, I.M. Sechenov First Moscow State Medical University, Moscow, Russia

Abstract

Studying the interaction of optical wavelength radiation with biological tissues can be used in various biomedical applications, including estimating the absorbed dose of laser radiation during laser-induced therapy. The fraction of absorbed radiation can be estimated using Monte Carlo and adding-doubling simulations. In this paper, we compare the simulation results obtained using the two methods for multilayered models of biological tissues of the trachea and colon. Both methods are used to calculate the absorbed dose based on the specified optical properties of tissues under several types of illumination. Similar incident beam geometries demonstrated repeatability of 94±3% for a collimated beam and 95±3% for an isotropic/diffuse source. The advantage of the adding-doubling method is its higher computational speed compared to the Monte Carlo method, while Monte Carlo simulation allows for varying a larger number of parameters when specifying the illumination conditions of the sample. The data obtained can be used to optimize dosimetry in photodynamic therapy.

Key words: optical property, adding-doubling method, Monte Carlo method, multilayer biological tissue, absorbed dose, laser dosimetry.

Contacts: Krivetskaya A.A., e-mail: annakrivetskaya1998@gmail.com

For citations: Krivetskaya A.A., Savelieva T.A., Kustov D.M., Levkin V.V., Kharnas S.S., Loschenov V.B. Investigation of methods for modeling light propagation in multilayer biological tissues for calculating the absorbed dose of laser radiation, *Biomedical Photonics*, 2026, vol. 15, no. 1, pp. 19–29. doi: 10.24931/2413–9432–2026–15-1-19-29

ИССЛЕДОВАНИЕ МЕТОДОВ МОДЕЛИРОВАНИЯ РАСПРОСТРАНЕНИЯ СВЕТА В МНОГОСЛОЙНЫХ БИОЛОГИЧЕСКИХ ТКАНЯХ ДЛЯ РАСЧЕТА ПОГЛОЩЕННОЙ ДОЗЫ ЛАЗЕРНОГО ИЗЛУЧЕНИЯ

А.А. Кривецкая[1,2], Т.А. Савельева[1,2], Д.М. Кустов[1], В.В. Левкин[3], С.С. Харнас[3], В.Б. Лощенов[1,2]
[1]Институт общей физики им. А.М. Прохорова Российской академии наук, Москва, Россия
[2]Национальный исследовательский ядерный университет «МИФИ», Москва, Россия
[3]Университетская Клиническая больница №1 Первого МГМУ им. Сеченова, Москва, Россия

Резюме

Изучение процессов взаимодействия излучения в оптическом диапазоне длин волн с биологическими тканями может применяться для различных биомедицинских применений, в том числе для оценки поглощенной дозы лазерного излучения при проведении лазерно-индуцированной терапии. Оценка доли поглощенного излучения может осуществляться при помощи моделирования методами Монте-Карло и удвоения-добавления. В данной работе проведен сравнительный анализ результатов моделирования двумя методами для многослойных моделей биологических тканей трахеи и толстой кишки. Оба метода применены для расчета поглощенной дозы по заданным оптическим свойствам тканей при нескольких видах освещения. Схожие геометрии пучка падающего излучения показали повторяемость с точностью 94±3% для коллимированного пучка и 95±3% для изотропного/диффузного источника. Преимуществом метода удвоения-добавления является большая вычислительная скорость по сравнению с методом Монте-Карло, в то

время как при моделировании методом Монте-Карло можно варьировать большее количество параметров при задании условий освещения образца. Полученные данные могут использоваться для оптимизации дозиметрии в фотодинамической терапии.

Ключевые слова: оптическое свойство, метод удвоения-добавления, метод Монте-Карло, многослойная биологическая ткань, поглощенная доза, лазерная дозиметрия.

Контакты: Кривецкая А.А., e-mail: annakrivetskaya1998@gmail.com

Для цитирования: Кривецкая А.А., Савельева Т.А., Кустов Д.М., Левкин В.В., Харнас С.С., Лощенов В.Б. Исследование методов моделирования распространения света в многослойных биологических тканях для расчета поглощенной дозы лазерного излучения // Biomedical Photonics. – 2026. –Т. 15, № 1. – С. 19–29. doi: 10.24931/2413–9432–2026–15-1-19-29

Introduction

In biomedical optics, the results of researches on modeling the propagation of light in biological tissues can be used for various biomedical applications, such as spectral diagnostics of photodynamic therapy, optical biopsy and monitoring of tissue oxygenation (StO_2), as well as for predicting the absorbed dose of laser radiation during laser-induced therapy [1, 2]. For a more accurate description of the interaction processes of optical radiation with real tissues, it is necessary to take into account their multilayeredness, since the optical properties of different layers can vary significantly, which reduces accuracy if the tissue is considered homogeneous.

Light propagation in tissue is determined by the optical properties of the medium: the absorption coefficient (μ_a), the scattering coefficient (μ_s), and the anisotropy factor (g). The absorption coefficient determines the probability of photon absorption per unit path length in the tissue. The main absorbers in biological tissues are hemoglobin, water, lipids, and melanin [3]. The scattering coefficient describes how often a photon changes direction in a medium. In the ultraviolet and far-infrared ranges, the contribution of scattering is relatively smaller compared to intense absorption. In the spectral range of 650-1000 nm, scattering dominates over absorption, creating the biological transparency window – the range in which optical radiation penetrates most deeply into biological tissue [4, 5]. The anisotropy factor (the average cosine of the scattering angle) determines the direction of light scattering.

Light propagation in biological tissues, which are turbid, i.e., highly scattering, media, can be described using radiative transfer theory. This theory ignores certain wave properties of light, such as interference and polarization, and considers only the transfer of light energy in the medium. It is assumed that the particle energy remains unchanged on average during interaction, and the analysis is limited to studying the propagation of monochromatic photons. The fundamental equation of radiative transfer theory incorporates the optical properties of the medium (μ_a and μs). Spectral measurements of multilayered biological tissues can yield values for parameters such as diffuse reflectance (R_d) and transmittance (T_d), whose values are determined by the optical properties of the object being studied and the measurement conditions.

Various approximations are used to solve the equations of radiative transfer theory. One of the standard methods for numerical solution is the Monte Carlo (MC) method [6, 7], which provides high accuracy due to stochastic modeling of photon trajectories, allows for the presence of layers with different values of optical properties to be taken into account, but requires significant computing resources and, accordingly, time costs [8]. An exact solution to the radiative transfer equation in biological tissues is only possible numerically, making the Monte Carlo method one of the most widely available and accurate tools for modeling diffuse reflectance and transmittance. The Monte Carlo method can be used both to solve the direct problem – modeling the diffuse reflectance and transmittance of a three-layer model of biological tissue based on given optical properties – and to solve the inverse problem – reconstructing optical properties based on diffuse reflectance and transmittance values [9]. A series of papers, including the first examples of simulating diffuse reflectance from a semi-infinite scattering medium and subsequent scalable methods for multilayer geometries, showed that the Monte Carlo method can take into account arbitrary distributions of μ_a, μ_s, and g, as well as complex geometries and illumination conditions [10]. In particular, photon trajectory scaling methods can significantly reduce calculation time for a wide range of optical parameters [11].

The adding-doubling (A-D) method can also be used to account for the multilayer nature of biological tissues. It allows for the rapid calculation of integrated reflectance and transmittance coefficients for layered media using the reflectance and transmittance matrices of individual layers. Due to its high speed, the A-D method is widely used to describe the light field in multilayered tissues and validate more complex models. However, the classical A-D method assumes the homogeneity of each layer and does not account for local inclusions. It is also limited in its analysis of the spatiotemporal structure of

the field, which limits its application in problems with strong heterogeneity [12, 13].

Systematic comparative studies of the effects of layers with different μ_a, μ_s, and g on diffuse reflectance and transmittance in multilayer fabrics are scarce. Based on publicly available data, there is only one study comparing Monte Carlo and adding-doubling methods for a single-layer sample [14]. In this paper, the results of modeling diffuse reflection and transmission in models of multilayer biological tissues using Monte Carlo and adding-doubling methods are compared.

Materials and methods

Algorithms describing the propagation of light in multilayer highly scattering media

The Monte Carlo method is one of the most frequently used methods for numerically solving the equation of radiative transfer theory. It involves determining the trajectory of a photon in a medium before it is absorbed or exits the medium based on the probabilities of absorption, scattering, and the scattering angle. These probabilities are determined by the optical properties of the medium – the absorption and scattering coefficients, as well as the anisotropy factor. Monte Carlo simulation of light propagation in tissue was performed for various incident beam geometries: from a point downward, from a point isotropically, from a fiber with a radius of 0.125 mm and an numerical aperture (NA) of 0.37, a collimated beam with a radius of 0.125 mm, and a Gaussian beam with a radius of 0.125 mm. A schematic representation of these incident beam geometries is shown in Fig. 1. In addition to the values of diffuse reflection and transmission, the Monte Carlo method makes it possible to determine the values of the fraction of absorbed radiation, which can be used to estimate the absorbed dose of laser radiation during laser-induced therapy.

The adding-doubling method can also be used to solve the radiative transfer equation. It was proposed by van de Hulst in 1963. The algorithm, as its name suggests, consists of two parts. First, for each set of optical properties corresponding to different layers in the sample, a "doubling" process is performed. In the first step, the diffuse reflectance (R_d) and transmittance (T_d) values are calculated for a thin layer whose thickness allows for only single scattering. The thickness is then doubled, and the R_d and T_d values are determined for the new thickness. This process is repeated until the final thickness of the layer with a given set of optical properties is reached. After the "doubling" process is complete for each set of optical properties, an "addition" process is performed, which involves calculating the diffuse reflectance and transmittance values for the entire sample, including layers with different sets of optical properties. To simulate the diffuse reflection and transmission of a multilayer models of biological tissues based on given optical properties, an algorithm was used, implemented in the Python programming language using the numpy, scipy, and iadpython libraries developed by Scott Prahl [15]. Light propagation in tissue was simulated for two incident beam geometries: collimated and diffuse. The fraction of absorbed radiation (A) was determined as $A = 1 - R_d - T_d$.

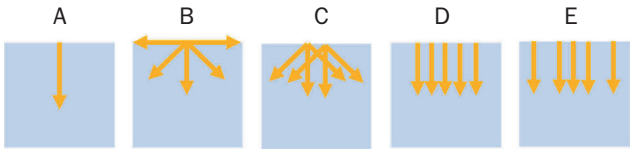

Рис. 1. Варианты геометрии падающего излучения при попадании света в ткань до взаимодействия с рассеивателями и поглотителями: A – из точки вниз; B – из точки изотропно; C – из волокна с заданным радиусом и апертурой; D – коллимированный пучок заданного радиуса; E – гауссов пучок заданного радиуса.
Fig. 1. Geometry options for incident radiation when light enters the tissue before interacting with diffusers and absorbers: A – from a point downwards; B – from a point isotropically; C – from a fiber with a given radius and aperture; D – collimated beam of a given radius; E – Gaussian beam of a given radius.

Mathematical models of multilayer media

In this study, the walls of hollow organs, such as the trachea and colon, were chosen as examples of multilayered tissues to allow considering different illumination conditions. Absorbed dose dosimetry is a practically significant task, for example, for the personalization of the photodynamic therapy (PDT) of the organs of the gastrointestinal tract, which performs for the treatment of gastrointestinal cancers as an adjunct to surgery, as well as for small tumors and as a palliative treatment [17-19]. As for trachea, secondary neoplasms of this organ are more common than primary tracheal tumors and typically arise from direct invasion of the trachea from primary malignancies in adjacent structures, such as the thyroid gland, lungs, esophagus, head and neck, or larynx. Examples of the effective use of PDT exist for such cases [20, 21], as well as for primary tumors of the trachea [22].

To achieve the objectives of this study, several models of highly scattering media were proposed. First, to compare and verify the modeling results, a single-layer model with optical properties on average relevant to the biological tissues proposed for study (trachea and intestine) was proposed. More complex models were constructed taking into account increasingly accurate representations of the layers in the walls of these hollow organs. Their geometries, optical properties and thickness (d) are presented in Tables 1-5.

To perform the simulation, the tracheal wall was represented as a four or six layer structure with specified optical properties and thicknesses. The parameters for each layer, for which the simulation was performed, such

Таблица 1
Оптические свойства однослойной модели биологических тканей

Table 1
Optical properties of a single-layer model of biological tissues

Параметр Parameter	Значения Values
μ_a, cm^{-1}	3
μ_s, cm^{-1}	130
g	0.77
n	1.38
d, mm	2

Таблица 2
Оптические свойства слоев модели биологической ткани, имитирующей слой надхрящницы трахеи между слизистыми на длине волны 542 нм

Table 2
Optical properties of the layers of the biological tissue model simulating the perichondrium layer of the trachea between the mucosal membranes at a wavelength of 542 nm

Параметр Parameter	Слои 1, 3 (слизистая) Layers 1, 3 (mucosa)	Слой 2 (надхрящница) Layer 2 (perichondrium)
μ_a, cm^{-1}	3.6	6.81
μ_s, cm^{-1}	142	120
g	0.73	0.79
n	1.38	1.38
d, mm	0.45	0.1

Таблица 3
Оптические свойства четырехслойной модели трахеи

Table 3
Optical properties of the four-layer trachea model

Слои Layers	Толщина слоя, мм Layer thickness, mm	μ_a, cm^{-1}, μ_s, cm^{-1}, g	542 nm	630 nm
слизистая mucosa	0.35	μ_a	3.6	2
		μ_s	142	139
		g	0.73	0.78
подслизистая submucosa	0.55	μ_a	2.8	1.6
		μ_s	140	138
		g	0.72	0.77
фиброзно - хрящевая оболочка fibrocartilaginous membrane	1	μ_a	4	1.1
		μ_s	120	117
		g	0.79	0.81
адвентиция adventitia	0.1	μ_a	3.5	1.4
		μ_s	78	70
		g	0.86	0.89

as thickness, scattering and absorption coefficients, and the anisotropy factor, are presented in Tables 3 and 4 [23–28]. The refractive index for all layers was taken equal to 1.37 [29, 30].

The normal colonic wall thickness ranges from 0 to 2 mm in colonic segments ≥4–6 cm in diameter, from 0.2 to 2.5 mm in colonic segments 3–4 cm in diameter, from 0.3 to 4 mm in colonic segments 2–3 cm in diameter, and from 0.5 to 5 mm in colonic segments 1–2 cm in diameter. The maximum colonic wall thickness reaches 6 and 8 mm in the proximal and distal colon, respectively, if the measured colonic segment demonstrated a lumen width <1 cm [31].

In work [32], measurements were made on 13 human colon samples (adenomal and normal sample in each case) for four tissue types (mucosa/submucosa and muscularis/chorion) using two integrating spheres and laser sources at wavelengths from 476.5 to 532 nm. Optical properties were assessed using the adding-doubling method. For normal tissues at a wavelength of

Таблица 4
Оптические свойства шестислойной модели трахеи

Table 4
Optical properties of the six-layer trachea model

Слои Layers	Толщина слоя, мм Layer thickness, mm	μ_a, cm^{-1}, µs, cm^{-1}, g	542 nm	630 nm
слизистая mucosa	0.35	μ_a	3.6	2
		μ_s	142	139
		g	0.73	0.78
подслизистая submucosa	0.55	μ_a	2.8	1.6
		μ_s	140	138
		g	0.72	0.77
фиброзно - хрящевая оболочка fibrocartilaginous membrane 1 mm	надхрящница perichondrium 0.1	μ_a oxyg.	6.81	1.12
		μ_a deox.	6.54	1.36
		μ_s	120	117
		g	0.79	0.81
	0.8	μ_a	4	1.1
		μ_s	120	117
		g	0.79	0.81
	надхрящница perichondrium 0.1	μ_a oxyg.	6.81	1.12
		μ_a deox.	6.54	1.36
		μ_s	120	117
		g	0.79	0.81
адвентиция adventitia	0.1	μ_a	3.5	1.4
		μ_s	78	70
		g	0.86	0.89

532 nm, the optical properties of the layer containing the mucous and submucosa were represented by the values μ_a = 3.33±0.14 cm^{-1}, μ_s = 208±5.16 cm^{-1}, g = 0.908±0.029, and for the tissues of the muscular layer μ_a = 1.53±0.06 cm^{-1}, μ_s =193±5.05 cm^{-1}, g = 0.941±0.048.

In the work of the same group [33], the optical properties of normal and adenomatous human colon tissues were investigated in vitro at wavelengths of 630, 680, 720, 780, 850 and 890 nm using a titanium-sapphire laser and the inverse Monte Carlo method. For the normal mucosa/submucosa at a wavelength of 630 nm, the values of μ_a = 0.143±0.004 cm^{-1} and μ_s = 208±5.27 cm^{-1} were determined. For the normal muscular layer, μ_a = 0.0997±0.0025 cm^{-1} and μ_s = 203±5.08 cm^{-1}. For the muscular layer/chorion of the human colon, the scattering anisotropy coefficient g at 633 nm was not reported directly in the main study using the integrating sphere. Since the value of the considered parameter increases smoothly with wavelength, and such studies often use a helium-neon laser with a wavelength of 632.8–633 nm, other studies of colon tissue at 633 nm typically use anisotropy coefficients in the range g≈0.94–0.96 for muscular or highly scattering layers of the colon. Thus, a practical estimate for the muscular layer of the colon at 633 nm is g≈0.945±0.01 for normal tissue and slightly higher for adenomatous tissue, suggesting the same monotonic trend extrapolated from the range 532→633 nm.

In the article [34], 20 samples of human colon tissue (10 samples of mucosa and 10 samples of submucosa) were placed in a 0.9% aqueous NaCl solution after resection and stored in it for 8–12 h at a temperature of ~4°C before spectral measurements were carried out. Optical properties were determined using a spectrophotometer with an integrating sphere in the range of 350–2500 nm. To restore the optical properties, the inverse doubling-addition method was used to estimate the initial values, and the inverse Monte Carlo method was used for the final determination. As a result, approximations were obtained for the spectrum of the scattering coefficient of the mucosal membrane by the function $\mu_s(\lambda) = 138.896\lambda^{-3.443} + 14460\lambda^{-0.617}$ and the submucosa by the function $\mu_s(\lambda) = 125.725\lambda^{-3.594} + 999.947\lambda^{-0.368}$, where λ is wavelength in nanometers. This results in values of $\mu_s(\lambda)$ = 300.8 cm^{-1} for the mucosa and $\mu_s(\lambda)$ = 99.3 cm^{-1} for the submucosa at a wavelength of 532 nm, and $\mu_s(\lambda)$ = 270 cm^{-1} for the mucosa and $\mu_s(\lambda)$ = 93 cm^{-1} for the submucosa at a wavelength of 633 nm. This means that the scattering coefficient for the mucosa is approximately three times higher than for the submucosa. Approximations were also obtained for the anisotropy factor of the mucosa and submucosa: $g(\lambda) = 0.77 + 0.18\,[1 - \exp(-(\lambda - 378.7)/111.1)]$ and $g(\lambda) = 0.77 + 0.19\,[1 - \exp(-(\lambda - 380.4)/128.1)]$. The authors also showed that absorption in the mucosa is higher than in the submucosa.

In [35], an inverse adding-doubling method was used to rapidly estimate optical properties based on spectra in the range from 400 to 1000 nm for pre-frozen colon mucosa and early-stage adenocarcinoma samples. For healthy mucosa, the absorption coefficient was 2.5 cm^{-1} at 532 nm and 0.75 cm^{-1} at 633 nm, while the reduced scattering coefficient was 19 cm^{-1} and 15.5 cm^{-1}, respectively. The anisotropy factor at 532 nm was determined to be 0.82, and at 633 nm, 0.865.

The refractive index of the tissues examined was taken from [36] and was 1.38 for mucosa, 1.36 for submucosa and muscle.

Combining the results of the works discussed above, we took for our mathematical model of the intestinal wall the values of optical properties presented in Table 5.

Таблица 5
Оптические параметры трехслойной модели нормальных тканей стенки толстой кишки

Table 5
Optical parameters of a three-layer model of normal colon wall tissues

Слои Layers	Толщина слоя, мм Layer thickness, mm	μ_a, cm^{-1}, μ_s, cm^{-1}, g	542 nm	630 nm
слизистая mucosa	0.4	μ_a	2,78	0,80
		μ_s	204,52	197,60
		g	0,88	0,90
		n	1,38	1,38
подслизистая submucosa	0.4	μ_a	1	0,7
		μ_s	99	93
		g	0,96	0,96
		n	1,36	1,36
мышечный слой muscular layer	2	μ_a	1,53	0,0997
		μ_s	193	203
		g	0,941	0,945
		n	1,36	1,36

Results and discussion

Results of mathematical modeling of light propagation in primary models

Tables 6 and 7 present for comparison the results of doubling-addition and Monte Carlo simulations for simplified models of biological tissues with optical properties in the range corresponding to real values at a wavelength of 542 nm.

The results of the Monte Carlo and adding-doubling algorithms show repeatability under similar illumination conditions (the isotropic source from a point for Monte Carlo can be compared with the diffuse illumination of the doubling-addition method, and the comparison of

conditions under collimated illumination requires no further comment).

Despite the fact that collimated incident beam is not an absolutely adequate model for experimental conditions under illumination through an optical fiber with a given aperture, we see from the Monte Carlo simulation results that these two illumination scenarios are still closer to each other than the isotropic/diffuse radiation source case. In the latter case, we obtain overestimated values for the diffuse reflectance signal.

Results of mathematical modeling of light propagation in trachea models

Tables 8–11 present the results of Monte Carlo and adding-doubling simulations of diffuse reflectance and transmittance values, as well as the fraction of absorbed radiation, for four-layer and six-layer tracheal models at wavelengths of 542 and 630 nm. Figure 2 shows a diagram of the light propagation trajectory in tissues during the recording of a diffuse reflectance and transmittance signal using the example of a four-layer trachea model.

When illuminated from the adventitia, diffuse reflection is expectedly lower due to light scattering, which is almost half as strong in the adventitia as in the mucosa. Moreover, the anisotropy factor is higher in the adventitia, meaning that for the scattering event the scattered photon is more likely to be directed forward, rather than backward, toward the diffuse reflectance signal receiver. This means that the mucosa acts as a kind of highly scattering mirror, reflecting light twice higher than adventitia.

For the six-layer tracheal model, a decrease in the agreement between the Monte Carlo and doubling-addition methods is observed (94±1%) compared to the four-layer model (95±2%). This is due to the fact that the six-layer model contains layers with a high level of

Таблица 6
Полученные путем моделирования распространения света в однослойной модели биологических тканей значения диффузного отражения и пропускания

Table 6
Diffuse reflection and transmission values obtained by simulating light propagation in a single-layer model of biological tissue

	MC	MC	MC	MC	MC	A-D	A-D
	NA 0.37	из точки вниз from a point downwards	изотропный isotropic	коллимированный collimated	Гауссов Gaussian	диффузный diffuse	коллимированный collimated
R_d	0.27	0.27	0.33	0.27	0.27	0.32	0.29
T_d	0.03	0.03	0.02	0.03	0.03	0.03	0.03

Таблица 7
Результаты моделирования для модели, представляющей собой надхрящницу трахеи между слизистыми

Table 7
Simulation results for a model representing the tracheal perichondrium between the mucous membranes

	MC	MC	MC	MC	MC	A-D	A-D
	NA 0.37	из точки вниз from a point downwards	изотропный isotropic	коллимированный collimated	Гауссов Gaussian	диффузный diffuse	коллимированный collimated
R_d	0.269	0.268	0.329	0.267	0.268	0.32	0.29
T_d	0.071	0.072	0.056	0.071	0.071	0.09	0.1

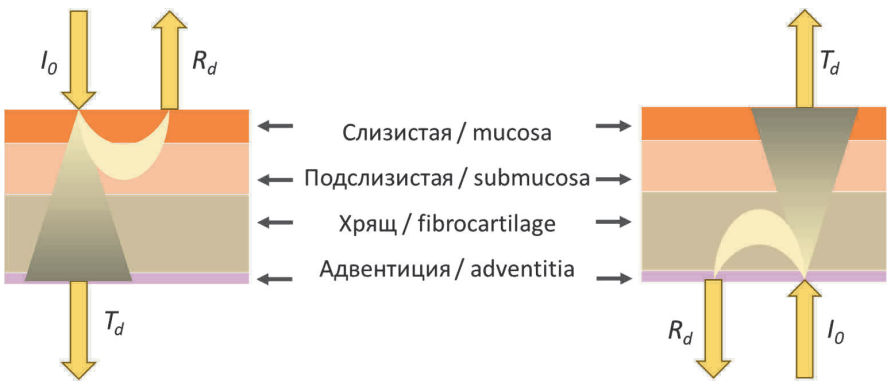

Рис. 2. Схема геометрии освещения (поток падающего излучения I0) и регистрации сигналов диффузного отражения (Rd) и диффузного пропускания (Td).
Fig. 2. Schematic diagram of the illumination geometry (incident radiation flux I0) and registration of diffuse reflection (Rd) and diffuse transmission (Td) signals.

Таблица 8
Результаты моделирования распространения излучения с длиной волны 542 нм в четырехслойной модели трахеи

Table 8
Results of modeling the propagation of radiation at a wavelength of 542 nm in a four-layer model of the trachea

Направление Direction		MC	MC	A-D	MC	A-D
		NA 0.37	диффузный diffuse		коллимированный collimated	
со стороны слизистой from the mucosa	R_d	0.287	0.343	0.351	0.286	0.302
	A	0.700	0.647	0.63	0.702	0.676
	T_d	0.013	0.010	0.019	0.013	0.022
со стороны адвентиции from the adventitia	R_d	0.166	0.216	0.246	0.164	0.212
	A	0.798	0.807	0.737	0.800	0.769
	T_d	0.035	0.027	0.017	0.035	0.019

Таблица 9
Результаты моделирования распространения излучения с длиной волны 630 нм в четырехслойной модели трахеи

Table 9
Results of modeling the propagation of radiation at a wavelength of 630 nm in a four-layer model of the trachea

Направление Direction		MC	MC	A-D	MC	A-D
		NA 0.37	диффузный diffuse		коллимированный collimated	
со стороны слизистой from the mucosa	R_d	0.35	0.40	0.402	0.35	0.369
	A	0.57	0.53	0.513	0.57	0.538
	T_d	0.08	0.06	0.085	0.08	0.093
со стороны адвентиции from the adventitia	R_d	0.30	0.34	0.408	0.29	0.377
	A	0.56	0.54	0.506	0.56	0.528
	T_d	0.14	0.11	0.086	0.14	0.095

Таблица 10
Результаты моделирования распространения излучения с длиной волны 542 нм в шестислойной модели трахеи

Table 10
Results of modeling the propagation of radiation with a wavelength of 542 nm in a six-layer model of the trachea

StO_2	Направление Direction		MC	MC	A-D	MC	A-D
			NA 0.37	диффузный diffuse		коллимированный collimated	
Оксигенированная надхрящница Oxygenated perichondrium	со стороны слизистой from the mucosa	R_d	0.287	0.342	0.340	0.285	0.306
		A	0.705	0.652	0.64	0.707	0.672
		T_d	0.008	0.006	0.020	0.008	0.022
	со стороны адвентиции from the adventitia	R_d	0.146	0.182	0.225	0.145	0.193
		A	0.830	0.801	0.76	0.831	0.79
		T_d	0.024	0.017	0.015	0.024	0.017
Дезоксигенированная надхрящница Deoxygenated perichondrium	со стороны слизистой from the mucosa	R_d	0.286	0.342	0.339	0.285	0.305
		A	0.705	0.651	0.644	0.707	0.675
		T_d	0.008	0.007	0.017	0.008	0.020
	со стороны адвентиции from the adventitia	R_d	0.148	0.184	0.227	0.147	0.195
		A	0.828	0.798	0.758	0.828	0.788
		T_d	0.024	0.018	0.015	0.025	0.017

blood filling (perichondrium), for which the absorption coefficient and the reduced scattering coefficient become closer, and the assumptions of the diffusion approximation of the radiative transfer theory no longer satisfy the conditions of light propagation [37]. Moreover, the modeling results differ to a greater extent when illuminated from the adventitia. This is explained by the fact that in this case the thin, but highly absorbing, perichondrium layer is closer to the source (in this case it is separated by only 0.1 mm of adventitia, as opposed to 0.9 mm of mucosa and submucosa in the case of illumination from the mucosa). Since the absorption of oxygenated hemoglobin at 630 nm is lower than that of free hemoglobin, these perichondrium layers, despite their blood supply, satisfy the conditions of the diffusion approximation and yield results closer to those of Monte Carlo simulation. Therefore, we can conclude that when a multilayered organ contains layers with a high absorption coefficient, Monte Carlo numerical simulation is preferable for calculating the absorbed dose. In other cases, the adding-doubling method provides results close to those of Monte Carlo simulation under similar illumination conditions.

Results of mathematical modeling of light propagation in a colon model

Tables 12 and 13 show the simulation results for the three-layer model of the colon wall.

Tables 12 and 13 shows that Monte Carlo simulations have a higher contrast between the recorded parameters of diffusely reflected and diffusely transmitted radiation for illumination from the mucosa and muscle compared to the adding-doubling simulations for a wavelength of 532 nm, while the opposite is true for 630 nm. Regardless of the simulation type, we see that the proportion of absorbed radiation is higher for illumination from the mucosa, which is clearly related to the fact that the more or less absorbing layer is located first in the path of the incident radiation, as it receives the higher radiation dose. However, the question is not what the total absorbed dose is across layers, but rather which layer is the focus of interest. If we consider the absorption by layers when illuminated with collimated light, then when illuminated at 630 nm from the mucosa, the mucosa will receive 0.146 of the total radiation, the submucosa 0.129, and the muscle 0.048. When illuminated at the same wavelength from the muscle side, the mucosa will absorb in fractions of 0.065, the submucosa 0.070, and the muscle 0.074. Thus, the best illumination option depends on the problem statement, since in the case of a neoplasm in the mucosal layer, it is logical to irradiate from this side, and in the presence of invasion into the muscle layer, we see that greater uniformity of the absorbed dose will be achieved when illuminating from this side.

During comparison of the absorbed radiation values for the trachea and colon models obtained using the Monte Carlo and adding-doubling methods, it was found that the methods considered show agreement with an accuracy of 95±3% (95±3% for the diffuse beam and 94±3% for the collimated beam).

Таблица 11
Результаты моделирования распространения излучения с длиной волны 630 нм в шестислойной модели трахеи

Table 11
Results of modeling the propagation of radiation with a wavelength of 630 nm in a six-layer model of the trachea

StO_2	Направление Direction		MC	MC	A-D	MC	A-D
			NA 0.37	диффузный diffuse		коллимированный collimated	
Оксигенированная надхрящница Oxygenated perichondrium	со стороны слизистой from the mucosa	R_d	0.352	0.405	0.413	0.350	0.381
		A	0.577	0.537	0.503	0.578	0.526
		T_d	0.071	0.058	0.084	0.071	0.093
	со стороны адвентиции from the adventitia	R_d	0.304	0.346	0.402	0.303	0.37
		A	0.567	0.549	0.512	0.567	0.535
		T_d	0.129	0.105	0.086	0.130	0.095
Дезоксигенированная надхрящница Deoxygenated perichondrium	со стороны слизистой from the mucosa	R_d	0.351	0.404	0.408	0.349	0.376
		A	0.580	0.539	0.509	0.581	0.533
		T_d	0.069	0.057	0.083	0.069	0.091
	со стороны адвентиции from the adventitia	R_d	0.298	0.340	0.402	0.297	0.369
		A	0.575	0.558	0.513	0.576	0.538
		T_d	0.127	0.103	0.085	0.127	0.093

Таблица 12
Результаты моделирования распространения излучения с длиной волны 532 нм в трехслойной модели стенки толстого кишечника

Table 12
Results of modeling the propagation of radiation at a wavelength of 532 nm in a three-layer model of the colonic wall

		MC	MC	A-D	MC	A-D
		NA 0.37	диффузный diffuse		коллимированный collimated	
со стороны слизистой from the mucosa	R_d	0.277	0.325	0.289	0.276	0.252
	A	0.684	0.643	0.632	0.685	0.66
	T_d	0.039	0.031	0.079	0.039	0.088
со стороны мышцы from the muscle	R_d	0.228	0.282	0.287	0.226	0.249
	A	0.676	0.643	0.637	0.677	0.666
	T_d	0.096	0.076	0.076	0.097	0.085

Таблица 13
Результаты моделирования распространения излучения с длиной волны 635 нм в трехслойной модели стенки толстого кишечника

Table 13
Results of modeling the propagation of radiation at a wavelength of 635 nm in a three-layer model of the colonic wall

		MC	MC	A-D	MC	A-D
		NA 0.37	диффузный diffuse		коллимированный collimated	
со стороны слизистой from the mucosa	R_d	0.471	0.514	0.457	0.470	0.425
	A	0.323	0.312	0.282	0.323	0.293
	T_d	0.206	0.174	0.261	0.206	0.282
со стороны мышцы from the muscle	R_d	0.484	0.544	0.543	0.482	0.509
	A	0.208	0.189	0.175	0.209	0.184
	T_d	0.308	0.267	0.282	0.309	0.307

Conclusion

Comparing Monte Carlo and adding-doubling methods for modeling light transport in multilayer biological tissues has great significance for the biomedical application of calculating the absorbed dose of laser radiation during various types of laser-induced therapies, such as hyperthermia or photodynamic therapy. These modeling methods represent fundamentally different approaches to solving the radiation transport problem. By comparing the results of Monte Carlo with those of the adding-doubling method in the same multilayer configuration, the numerical accuracy of the latter's implementations can be verified and the errors introduced by its assumptions can be quantified. The adding-doubling method uses an analytical approximation of radiation transfer theory, enabling rapid calculation of the required transmission, reflection, and absorption parameters. Monte Carlo, as a numerical simulation method, is computationally expensive but can naturally handle complex 3D geometries, heterogeneous layers, and arbitrary source and detector configurations.

In this article, we compared various implementations of these two methods for multilayer models of biological tissues such as the tracheal wall (with progressively more complex structure in the models) and the colon wall. We examined the influence of the illumination side of the multilayer tissue on the light propagation parameters, the effect of thin but blood-filled layers on light propagation, and the effect of the degree of blood oxygen saturation in the tissues. We demonstrated that for multilayer media with inclusions of layers containing blood at a such concentration that the absorption coefficient and the reduced scattering coefficient become sufficiently close that the assumptions of the diffusion approximation of radiative transfer theory do not satisfy the conditions for light propagation, the use of Monte Carlo numerical simulation is preferable for calculating the absorbed dose, while in other cases the adding-doubling method yields values of absorbed dose close to Monte Carlo results under similar illumination conditions.

The work was funded by the Russian Science Foundation, grant No. 25-25-00516.

REFERENCES

1. Star W.M. Light dosimetry in vivo. *Physics in medicine and biology,* 1997, vol. 42, pp. 763–787. doi: 10.1088/0031-9155/42/5/003
2. Wilson B.C., Lilge L., Weersink R.A., Pires L. Photodynamic therapy dosimetry: current status and the emerging challenge of immune stimulation. *Journal of biomedical optics,* 2025, vol. 30, pp. S34118. doi: 10.1117/1.JBO.30.S3.S34118
3. Bergmann F., Foschum F., Marzel L., Kienle A. Ex Vivo Determination of Broadband Absorption and Effective Scattering Coefficients of Porcine Tissue. *Photonics,* 2021, vol. 8, pp. 365. https://doi.org/10.3390/photonics8090365
4. Deyev S., Lebedenko E. Targeted Bifunctional Proteins and Hybrid Nanoconstructs for Cancer Diagnostics and Therapies. *Molecular Biology,* 2017, vol. 51, pp. 788-803. doi: 10.1134/S002689331706005X
5. Albraim S., Issa H., Alaissamy K., Bartoli A., Alhabeel M. Photodynamic Therapy in Skin Treatment. *Journal of MAR Dental Sciences,* 2022, vol. 7, p. 3.
6. Serebryakova I., Surkov Yu., Fashchevskii A., Xu Y., Xia Q., Li D., Zhu D., Genina E., Tuchin V. Monte Carlo simulation of light distribution in multilayer biological tissue. *Chinese-Russian workshop on biophotonics and biomedical optics-2024,* 2024, vol. 1, pp. 33-38. doi: 10.24412/cl-37303-2024-1-33-38
7. Savelieva T.A., Krivetskaya A.A., Kustov D.M., Klobukov M.I., Romanishkin I.D., Linkov K.G., Levkin V.V., Kharnas S.S., Loschenov V.B. Application of the Kubelka-Munk model for fast intraoperative analysis of intestinal optical properties using a fiber optic spectrometer. *Biomedical Photonics,* 2025, vol. 14, pp. 30-38. doi: 10.24931/2413-9432-2025-14-3-30-38
8. Romanishkin I.D., Savelieva T.A., Ospanov A., Kalyagina N.A., Krivetskaya A.A., Udeneev A.M., Linkov K.G., Goryajnov S.A., Shugay S.V., Pavlova G.V., Pronin I.N., Loschenov V.B. Comparison of optical-spectral characteristics of glioblastoma at intraoperative diagnosis and ex vivo optical biopsy. *Biomedical Photonics,* 2024, vol. 13, pp. 4-12. doi: 10.24931/2413-9432-2024-13-4-4-12
9. Fredriksson I., Larsson M., Strömberg T. Inverse Monte Carlo method in a multilayered tissue model for diffuse reflectance spectroscopy. *J. Biomed. Opt,* 2012, vol. 17, pp. 047004. doi: 10.1117/1.JBO.17.4.047004
10. Privalov V.E., Seteikin A.Yu., Fotiadi A.E. Simulation of laser radiation propagation in inhomogeneous media with complex geometry. *Научно-технические ведомости Санкт-Петербургского государственного политехнического университета. Физико-математические науки,* 2013, vol. 4-2, pp. 148-153.
11. Liu Q., Ramanujam N. Scaling method for fast Monte Carlo simulation of diffuse reflectance spectra from multilayered turbid media. *J. Opt. Soc. Am. A,* 2007, vol. 24, pp. 1011-1025.
12. Prahl S.A., van Gemert M.J.C., Welch A.J. Determining the optical properties of turbid media by using the adding–doubling method. *Appl. Opt,* 1993, vol. 32, pp. 559-568.
13. Prahl S.A. The Adding-Doubling Method. In: Welch A. J., Van Gemert M. J. C., eds. Optical-Thermal Response of Laser-Irradiated Tissue. *Lasers, Photonics, and Electro-Optics,* Springer, Boston, MA; 1995. doi: 10.1007/978-1-4757-6092-7_5
14. Vincely V.D., Vishwanath K. Lateral light losses in integrating sphere measurements: comparison of Monte-Carlo with inverse adding-doubling algorithm. *Proc. SPIE,* 2020, pp. 11231:112310G. doi: 10.1117/12.2546265
15. https://github.com/scottprahl/iadpython
16. Lee H.H., Choi M.G., Hasan T. Application of photodynamic therapy in gastrointestinal disorders: an outdated or re-emerging technique? *The Korean journal of internal medicine,* 2017, vol. 32, pp. 1–10. doi: 10.3904/kjim.2016.200
17. Tseimakh A.E., Shoykhet I.N., Tseimakh E.A., Bedyan N.K., Makarenkov A.S. Multi-course photodynamic therapy in a patient with malignant tumor of the major duodenal papilla. Clinical case. *Biomedical Photonics,* 2025, vol. 14, pp. 39-42. doi: 10.24931/2413-9432-2025-14-3-39-42;
18. Rodrigues J.A., Correia J.H. Photodynamic Therapy for Colorectal Cancer: An Update and a Look to the Future. *International Journal of Molecular Sciences,* 2023, vol. 24, pp. 12204. doi: 10.3390/ijms241512204
19. Krivetskaya A.A., Savelieva T.A., Kustov D.M., Levkin V.V., Kharnas S.S., Loschenov V.B. Automatization of planning and control of

ЛИТЕРАТУРА

1. Star W.M. Light dosimetry in vivo // Physics in medicine and biology. – 1997. – Vol. 42. – P. 763–787. doi: 10.1088/0031-9155/42/5/003.
2. Wilson B. C., Lilge L., Weersink R. A., Pires L. Photodynamic therapy dosimetry: current status and the emerging challenge of immune stimulation // Journal of biomedical optics. – 2025. – Vol. 30. – P. 34118. doi: 10.1117/1.JBO.30.S3.S34118.
3. Bergmann F., Foschum F., Marzel L., Kienle A. Ex Vivo Determination of Broadband Absorption and Effective Scattering Coefficients of Porcine Tissue // Photonics. – 2021. – Vol. 8. – P. 365. doi: 10.3390/photonics8090365.
4. Deyev S., Lebedenko E. Targeted Bifunctional Proteins and Hybrid Nanoconstructs for Cancer Diagnostics and Therapies // Molecular Biology. – 2017. – Vol. 51. – P. 788-803. doi: 10.1134/S002689331706005X.
5. Albraim S., Issa H., Alaissamy K., Bartoli A., Alhabeel M. Photodynamic Therapy in Skin Treatment // Journal of MAR Dental Sciences. – 2022. – Vol. 7. – P. 3.
6. Serebryakova I., Surkov Yu., Fashchevskii A., Xu Y., Xia Q., Li D., Zhu D., Genina E., Tuchin V. Monte Carlo simulation of light distribution in multilayer biological tissue // Китайско-российский семинар по биофотонике и биомедицинской оптике-2024. – 2024. – Vol. 1. – P. 33-38. doi: 10.24412/cl-37303-2024-1-33-38.
7. Савельева Т.А., Кривецкая А.А., Кустов Д.М., Клобуков М.И., Романишкин И.Д., Линьков К.Г., Левкин В.В., Харнас С.С., Лощенов В.Б. Применение модели Кубелки-Мунка для быстрого интраоперационного анализа оптических свойств стенки кишечника с помощью оптоволоконного спектрометра // Biomedical Photonics. –2025. –Vol. 14. – P. 30-38. doi: 10.24931/2413-9432-2025-14-3-30-38.
8. Романишкин И.Д., Савельева Т.А., Оспанов А., Калягина Н.А., Кривецкая А.А., Уденеев А.М., Линьков К.Г., Горяйнов С.А., Шугай С.В., Павлова Г.В., Пронин И.Н., Лощенов В.Б. Сравнение оптико-спектральных характеристик глиобластомы при интраоперационной диагностике и оптической биопсии *ex vivo* // Biomedical Photonics. –2024. – Vol. 13. – P. 4-12. doi: 10.24931/2413-9432-2024-13-4-4-12.
9. Fredriksson I., Larsson M., Strömberg T. Inverse Monte Carlo method in a multilayered tissue model for diffuse reflectance spectroscopy // J. Biomed. Opt. – 2012. –Vol. 17. – P. 047004. doi: 10.1117/1.JBO.17.4.047004.
10. Привалов В.Е., Сетейкин А.Ю., Фотиади А.Э. Моделирование распространения лазерного излучения в неоднородных средах со сложной геометрией. Научно-технические ведомости Санкт-Петербургского государственного политехнического университета // Физико-математические науки. – 2013. – Vol. 4-2. –P. 148-153.
11. Liu Q., Ramanujam N. Scaling method for fast Monte Carlo simulation of diffuse reflectance spectra from multilayered turbid media // J. Opt. Soc. Am. A. – 2007. – Vol. 24. – P. 1011-1025.
12. Prahl S.A., van Gemert M.J.C., Welch A.J. Determining the optical properties of turbid media by using the adding–doubling method // Appl. Opt. – 1993. – Vol. 32. – P. 559-568.
13. Prahl S.A. The Adding-Doubling Method. In: Welch A. J., Van Gemert M. J. C., eds. Optical-Thermal Response of Laser-Irradiated Tissue // Lasers, Photonics, and Electro-Optics. Springer, Boston, MA. – 1995. doi: 10.1007/978-1-4757-6092-7_5.
14. Vincely V.D., Vishwanath K. Lateral light losses in integrating sphere measurements: comparison of Monte-Carlo with inverse adding-doubling algorithm // Proc. SPIE. – 2020. – P. 11231:112310G. doi: 10.1117/12.2546265.
15. https://github.com/scottprahl/iadpython
16. Lee H.H., Choi M.G., Hasan T. Application of photodynamic therapy in gastrointestinal disorders: an outdated or re-emerging technique? // The Korean journal of internal medicine. – 2017. – Vol. 32. – P. 1–10. doi: 10.3904/kjim.2016.200.
17. Цеймах А.Е., Шойхет Я.Н., Цеймах Е.А., Бедян Н.К., Макаренков А.С. Многокурсовая фотодинамическая терапия у пациента со злокачественным новообразованием большого дуоденального сосочка. Клинический случай // Biomedical Photonics. – 2025. – Vol. 14. – P. 39-42. doi: 10.24931/2413-9432-2025-14-3-39-42.
18. Rodrigues J.A., Correia J.H. Photodynamic Therapy for Colorectal Cancer: An Update and a Look to the Future // International Journal of Molecular Sciences. – 2023. –Vol. 24. – P. 12204. doi: 10.3390/ijms241512204.
19. Кривецкая А.А., Савельева Т.А., Кустов Д.М., Левкин В.В., Харнас С.С., Лощенов В.Б. Автоматизация планирования и контроля фо-

photodynamic therapy of gastrointestinal organs. *Biomedical Photonics,* 2025, vol. 14, pp. 40-54. doi: 10.24931/2413-9432-2025-14-2-40-54

20. Singh H., Benn B.S., Jani C., Abdalla M., Kurman J.S. Photodynamic therapy for treatment of recurrent adenocarcinoma of the lung with tracheal oligometastasis. *Respiratory medicine case reports,* 2022, vol. 37, pp. 101620. doi: 10.1016/j.rmcr.2022.101620
21. Jung H.S., Kim H.J., Kim K.W. Intraoperative photodynamic therapy for tracheal mass in non-small cell lung cancer: A case report. *World journal of clinical cases,* 2023, vol. 11, pp. 3915–3920. doi: 10.12998/wjcc.v11.i16.3915
22. Martin L.K., Otterson G.A., Bekaii-Saab T. Photodynamic therapy (PDT) may provide effective palliation in the treatment of primary tracheal carcinoma: a small case series. *Photomedicine and laser surgery,* 2012, vol. 30, pp. 668–671. doi: 10.1089/pho.2012.3293
23. Hohmann M., Lengenfelder B., Kanawade R., Klämpfl F., Douplik A., Albrecht H. Measurement of optical properties of pig esophagus by using a modified spectrometer set-up. *Journal of Biophotonics,* 2017, vol. 11. doi: 10.1002/jbio.201600187
24. Descalle M.-A., Jacques S.L., Prahl S.A., Laing T.J., Martin W.R. Measurements of ligament and cartilage optical properties at 35mm, 365nm and in the visible range [440-800nm]. *SPIE,* 1998, vol. 3195, pp. 280-286.
25. Youn J.-I., Telenkov S.A., Kim E., Bhavaraju N.C., Wong B.J.F., Valvano J. W., Milner T. E. Optical and Thermal Properties of Nasal Septal Cartilage. *Lasers in Surgery and Medicine,* 2000, vol. 27, pp. 119-128.
26. Bagratashvili N.V., Sviridov A.P., Sobol E.N., Kitai M.S. Optical properties of nasal septum cartilage. *Proc. SPIE,* 1998, vol. 3254. doi: 10.1117/12.308189
27. Nawn C.D., Blackburn M.B., De Lorenzo R.A., Ryan K.L. Using spectral reflectance to distinguish between tracheal and oesophageal tissue: applications for airway management. *Anaesthesia,* 2019, vol. 74, pp. 340-347. doi: 10.1111/anae.14566
28. Ebert D., Roberts C., Farrar S., Johnston W., Litsky A., Bertone A. Articular Cartilage Optical Properties in the Spectral Range 300-850 nm. *Journal of biomedical optics,* 1998, vol. 3, pp. 326-33. doi: 10.1117/1.429893
29. Khan R., Gul B., Khan S., Nisar H., Ahmad I. Refractive index of biological tissues: Review, measurement techniques, and applications. *Photodiagnosis and photodynamic therapy,* 2021, vol. 33, pp. 102192. doi: 10.1016/j.pdpdt.2021.102192
30. Carvalho S., Gueiral N., Nogueira E., Henrique R., Oliveira L., Tuchin V. Wavelength dependence of the refractive index of human colorectal tissues: comparison between healthy mucosa and cancer. *Journal of Biomedical Photonics & Engineering,* 2016, vol. 2, pp. 040307-1. doi: 10.18287/JBPE16.02.040307
31. Wiesner W., Mortelé K. J., Ji H., Ros P. R. Normal colonic wall thickness at CT and its relation to colonic distension. *Journal of computer assisted tomography,* 2002, vol. 26, pp. 102–106. doi: 10.1097/00004728-200201000-00015
32. Wei H.J., Xing D., Lu J.J., Gu H.M., Wu G.Y., Jin Y. Determination of optical properties of normal and adenomatous human colon tissues in vitro using integrating sphere techniques. *World journal of gastroenterology,* 2005, vol. 11, pp. 2413–2419. doi: 10.3748/wjg.v11.i16.2413
33. Wei H., Xing D., Wu G., Gu H., Lu J., Jin Y., Li X.-Y. Differences in optical properties between healthy and pathological human colon tissues using a Ti:sapphire laser: an in vitro study using the Monte Carlo inversion technique. *J. Biomed. Opt,* 2005, vol. 10, pp. 044022. doi: 10.1117/1.1990125
34. Bashkatov A., Genina E., Kochubey V., Rubtsov V., Kolesnikova E., Tuchin V. Optical properties of human colon tissues in the 350–2500 nm spectral range. *Quantum Electronics,* 2014, vol. 44, pp. 77. doi: 10.1070/QE2014v044n08ABEH015613
35. Carvalho S., Gueiral N., Nogueira E., Henrique R., Oliveira L., Tuchin V. V. Comparative study of the optical properties of colon mucosa and colon precancerous polyps between 400 and 1000 nm. *Proc. SPIE,* 2017, pp. 10063:100631L. doi: 10.1117/12.2253023
36. Vo-Dinh T., ed. *Biomedical Photonics Handbook,* 1st ed. CRC Press; 2003. doi: 10.1201/9780203008997
37. Ismael F.S., Amasha H.M., Bachir W.H. A diffusion equation based algorithm for determination of the optimal number of fibers used for breast cancer treatment planning in photodynamic therapy. *Biomedical Photonics,* 2019, vol. 8, pp. 17-27. doi: 10.24931/2413-9432-2019-8-4-17-27

тодинамической терапии органов желудочно-кишечного тракта // Biomedical Photonics. – 2025. – 14. – P. 40-54. doi: 10.24931/2413-9432-2025-14-2-40-54.

20. Singh H., Benn B.S., Jani C., Abdalla M., Kurman J.S. Photodynamic therapy for treatment of recurrent adenocarcinoma of the lung with tracheal oligometastasis // Respiratory medicine case reports. – 2022. – Vol. 37. – P. 101620. doi: 10.1016/j.rmcr.2022.101620.
21. Jung H.S., Kim H.J., Kim K.W. Intraoperative photodynamic therapy for tracheal mass in non-small cell lung cancer: A case report // World journal of clinical cases. – 2023. – Vol. 11. – P. 3915–3920. https://doi.org/10.12998/wjcc.v11.i16.3915.
22. Martin L.K., Otterson G.A., Bekaii-Saab T. Photodynamic therapy (PDT) may provide effective palliation in the treatment of primary tracheal carcinoma: a small case series // Photomedicine and laser surgery. – 2012. – Vol. 30. – P. 668–671. doi: 10.1089/pho.2012.3293.
23. Hohmann M., Lengenfelder B., Kanawade R., Klämpfl F., Douplik A., Albrecht H. Measurement of optical properties of pig esophagus by using a modified spectrometer set-up // Journal of Biophotonics. – 2017. – Vol. 11. doi: 10.1002/jbio.201600187.
24. Descalle M.-A., Jacques S.L., Prahl S.A., Laing T.J., Martin W.R. Measurements of ligament and cartilage optical properties at 35mm, 365nm and in the visible range [440-800nm] // SPIE. – 1998. – Vol. 3195. – P. 280-286.
25. Youn J.-I., Telenkov S. A., Kim E., Bhavaraju N. C., Wong B. J. F., Valvano J. W., Milner T. E. Optical and Thermal Properties of Nasal Septal Cartilage // Lasers in Surgery and Medicine. – 2000. – Vol. 27. – P. 119-128.
26. Bagratashvili N.V., Sviridov A.P., Sobol E.N., Kitai M.S. Optical properties of nasal septum cartilage // Proc. SPIE. – 1998. – P.3254. https://doi.org/10.1117/12.308189.
27. Nawn C.D., Blackburn M.B., De Lorenzo R.A., Ryan K.L. Using spectral reflectance to distinguish between tracheal and oesophageal tissue: applications for airway management // Anaesthesia. – 2019. – Vol. 74. – P. 340-347. doi: 10.1111/anae.14566.
28. Ebert D., Roberts C., Farrar S., Johnston W., Litsky A., Bertone A. Articular Cartilage Optical Properties in the Spectral Range 300-850 nm // Journal of biomedical optics. – 1998. – Vol. 3. – P. 326-33. doi: 10.1117/1.429893.
29. Khan R., Gul B., Khan S., Nisar H., Ahmad I. Refractive index of biological tissues: Review, measurement techniques, and applications // Photodiagnosis and photodynamic therapy. – 2021. – Vol. 33. – P. 102192. doi: 10.1016/j.pdpdt.2021.102192.
30. Carvalho S., Gueiral N., Nogueira E., Henrique R., Oliveira L., Tuchin V. Wavelength dependence of the refractive index of human colorectal tissues: comparison between healthy mucosa and cancer // Journal of Biomedical Photonics & Engineering. – 2016. – Vol. 2. – P. 040307-1. doi: 10.18287/JBPE16.02.040307.
31. Wiesner W., Mortelé K.J., Ji H., Ros P.R. Normal colonic wall thickness at CT and its relation to colonic distension // Journal of computer assisted tomography. – 2002. – Vol. 26. – P. 102–106. doi: 10.1097/00004728-200201000-00015.
32. Wei H.J., Xing D., Lu J.J., Gu H.M., Wu G.Y., Jin Y. Determination of optical properties of normal and adenomatous human colon tissues in vitro using integrating sphere techniques // World journal of gastroenterology. – 2005. – Vol. 11. – P. 2413–2419. doi: 10.3748/wjg.v11.i16.2413.
33. Wei H., Xing D., Wu G., Gu H., Lu J., Jin Y., Li X.-Y. Differences in optical properties between healthy and pathological human colon tissues using a Ti:sapphire laser: an in vitro study using the Monte Carlo inversion technique // J. Biomed. Opt. – 2005. – Vol. 10. – P. 044022. doi: 10.1117/1.1990125.
34. Bashkatov A., Genina E., Kochubey V., Rubtsov V., Kolesnikova E., Tuchin V. Optical properties of human colon tissues in the 350–2500 nm spectral range // Quantum Electronics. – 2014. – Vol. 44. – P. 77. doi: 10.1070/QE2014v044n08ABEH015613.
35. Carvalho S., Gueiral N., Nogueira E., Henrique R., Oliveira L., Tuchin V.V. Comparative study of the optical properties of colon mucosa and colon precancerous polyps between 400 and 1000 nm // Proc. SPIE. – 2017. – P. 10063:100631L. doi: 10.1117/12.2253023.
36. Vo-Dinh T., ed. Biomedical Photonics Handbook. 1st ed. CRC Press. – 2003. doi: 10.1201/9780203008997.
37. Ismael F.S., Amasha H.M., Bachir W.H. Алгоритм определения оптимального числа волокон используемых при внутритканевой фотодинамической терапии рака молочной железы на основании диффузионного уравнения // Biomedical Photonics. – 2019. – Vol. 8. – P. 17-27. doi: 10.24931/2413-9432-2019-8-4-17-27